DALTON

# Formation of $[CoPt_2Cl_2(PPh_3)_4(\mu_3\text{-}S)_2]$ from facile heterometallation of $[Pt_2(PPh_3)_4(\mu\text{-}S)_2]$ and its facile deheterometallation *via* carbonylative desulfurization to give Pt–Pt bonded $[Pt_2(CO)_2(PPh_3)_2(\mu\text{-}S)]$ †

**Huang Liu,[a] Agnes L. Tan,[b] Kum F. Mok *,[a] and T. S. Andy Hor *,[a]**

[a] *Department of Chemistry, Faculty of Science, National University of Singapore, Kent Ridge, 119260, Singapore*

[b] *Department of Computational Science, Faculty of Science, National University of Singapore, Kent Ridge, 119260, Singapore*

Metallation of $[Pt_2(PPh_3)_4(\mu\text{-}S)_2]$ **1** with $CoCl_2$ gave $[CoPt_2Cl_2(PPh_3)_4(\mu_3\text{-}S)_2]$ **2** at room temperature. Treatment of **2** with CO in an autoclave resulted in a binuclear compound $[Pt_2(CO)_2(PPh_3)_2(\mu\text{-}S)]$ **3**, *via* a reductive desulfurization mechanism with the removal of the heterometal fragment and formation of a Pt–Pt bond. Complexes **2** and **3** have been characterized by single-crystal X-ray crystallography. The structure of **2** shows a trigonal-bipyramidal arrangement of a $\{CoPt_2S_2\}$ core with non-bonding Pt–Pt and Co–Pt distances at 3.197(4) and 3.066(1) Å respectively. Complex **3** contains a $\{Pt_2S\}$ trinagular core with two $PPh_3$ ligands *trans* and two CO *cis* to the Pt–Pt bond [2.600(1) Å]. Some theoretical aspects of the strength of the Pt–Pt bond in relation to the ligands on the $\{Pt_2S\}$ core are discussed.

The ability of $[Pt_2(PPh_3)_4(\mu\text{-}S)_2]$ **1** to function as a metalloligand towards a variety of heavy-metal fragments (*e.g.* $Rh^I$,[1] $Pd^{II}$ [2], $Pt^{II}$,[3] $Ag^I$,[4] $Au^I$ [5]) has been structurally established. This form of Lewis acid–base addition represents simple yet powerful means to enter into platinum heterometallic polynuclear sulfide complexes. Such addition, which has been extended to the p-block metals,[6,7] in principle can be applied also to the smaller first-row transition metals. However, to date only spectroscopic evidence is available for such addition.[2,8] Among the heterometallic complexes isolated, most of the Lewis acids contain 'soft' ligands such as $C_2H_4$ and $PPh_3$, which tend to raise the electrophilicity of the heterometals and strengthen the Lewis acid–base binding. In this paper, we furnish evidence that a classical 3d-metal compound such as $CoCl_2$ can exhibit similar activity towards complex **1** but that the resultant triangular complex collapses under mild carbon monoxide pressure through a reductive desulfurization mechanism to give a homometallic Pt–Pt bonded dimer $[Pt_2(CO)_2(PPh_3)_2(\mu\text{-}S)]$ **3**.

## Results and Discussion

Addition reaction occurs rapidly between equimolar amounts of anhydrous $CoCl_2$ and complex **1** in tetrahydrofuran (thf) to give a clear yellowish green solution from which $[CoPt_2Cl_2(PPh_3)_4(\mu_3\text{-}S)_2]$ **2** can be isolated. The use of the hydrated form $CoCl_2{\cdot}6H_2O$ would also yield **2** but it readily decomposes upon formation. Conductivity data for **2** suggest a non-electrolyte in $CH_2Cl_2$ solution. The $^{31}P$ NMR spectrum suggests the phosphines to be chemically equivalent. The magnetic moment (4.79 $\mu_B$) is consistent with a high-spin tetrahedral $d^7$ cobalt(II) complex.[9] Treating **2** under a mild pressure of CO (45 psi) in an autoclave at 80 °C for 24 h gives $[Pt_2(CO)_2(PPh_3)_2(\mu\text{-}S)]$ **3** and an unidentified cobalt compound (Scheme 1). Complex **3** has been previously obtained from a similar reductive desulfurization of **1** under mild carbon monoxide pressure[10] and from a cluster degradation of $[Pt_3(PPh_3)_2(\mu\text{-}CO)_3]$ by COS.[11] However, there has been no crystallographic report of **3**. Its parent complex $[Pt_2(CO)_4(\mu\text{-}S)]$ is unknown and $[Pt_2(PPh_3)_4(\mu\text{-}S)]$[10,12] is not well established. The monocarbonyl derivative $[Pt_2(CO)(PPh_3)_3(\mu\text{-}S)]$ **4**, obtained from $[Pt(PPh_3)_3]$ with COS[13] or from **3** with $PPh_3$,[10] was the first crystallographically characterized example which shows a Pt–S–Pt triangular core.

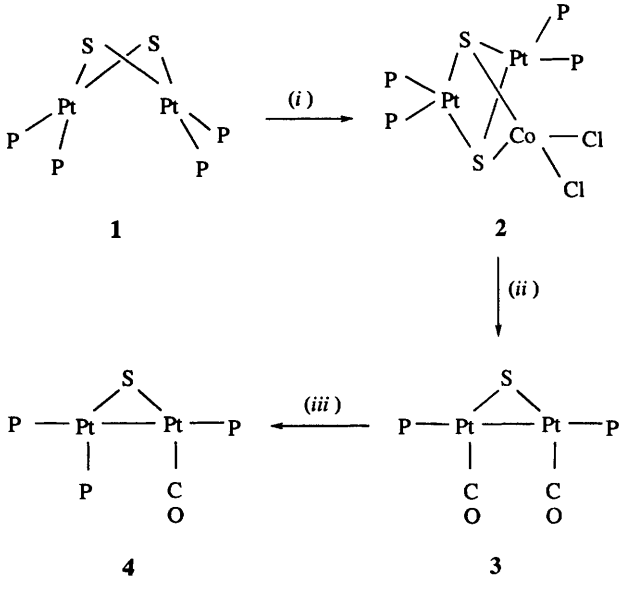


**Scheme 1** P = $PPh_3$. (*i*) $CoCl_2$, room temperature; (*ii*) 45 psi CO, heat; (*iii*) $PPh_3$

Both complexes **2** and **3** were characterized by single-crystal X-ray diffractometry. Complex **2** shows an addition of $CoCl_2$ across the S···S axis of **1** resulting in a $\{CoPt_2S_2\}$ trigonal-bipyramidal molecular core (Table 1 and Fig. 1). The formation of a stable tetrahedral $d^7$ cobalt(II) complex, which is paramagnetic, is attributed largely to the polarizability of the sulfur donors and steric shielding imposed by **1** in a chelating mode. No direct metal–metal bonding is envisaged for 16-electron square-planar platinum(II) complexes [Pt···Pt average 3.197(4) Å]. The Co···Pt distances in **2** [average 3.066(1) Å] are significantly longer than the carbonyl-bridged Co–Pt bonds [2.599(2)–2.661(2) Å] but comparable to the unbridged Co–Pt bonds [2.937(2)–3.060(2) Å] in a hexanuclear cluster $[Co_3Pt_3$-

† *Non-SI units employed:* $\mu_B \approx 9.27 \times 10^{-24}$ J $T^{-1}$, psi $\approx 6.89 \times 10^3$ Pa.

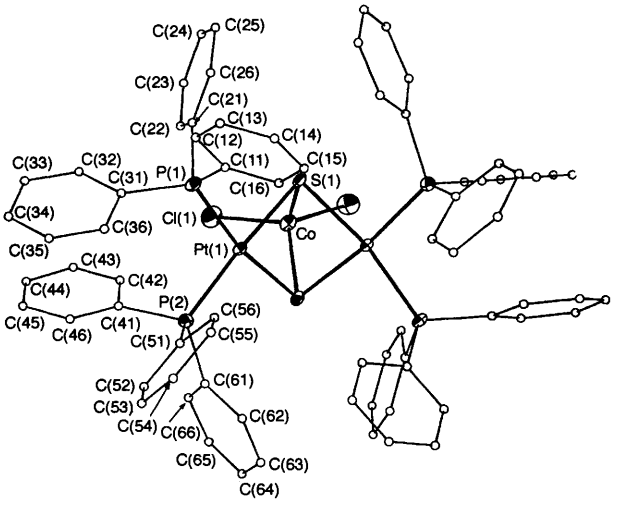


**Fig. 1** Perspective view of $[CoPt_2Cl_2(PPh_3)_4(\mu_3\text{-}S)_2]$ **2** at the 20% probability level

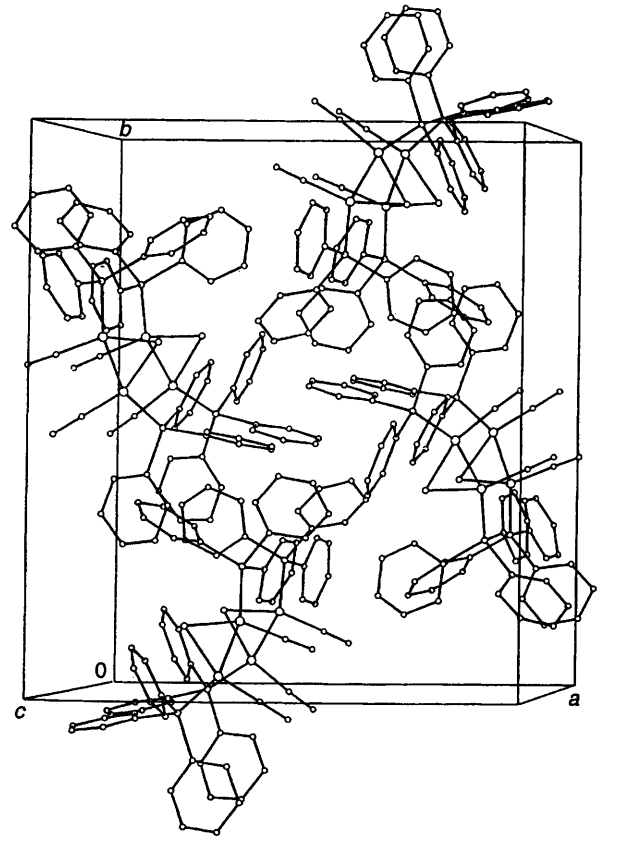


**Fig. 2** Crystal packing of $[Pt_2(CO)_2(PPh_3)_2(\mu\text{-}S)]$ **3**, showing two crystallographically distinct molecules in a unit cell

$(\mu\text{-}CO)_4(CO)_5(PPr^i_3)_3(\mu_6\text{-}C)(\mu\text{-}H)]$.[14] The Pt–S bond [average 2.345(3) Å] is within expectation,[1–5] but the Co–S bond [2.359(4) Å] is weaker than the Co–$(\mu_3$-S) bond [average 2.234(6) Å] found in $[Co_6(PEt_3)_6(\mu_3\text{-}S)_8][BPh_4]$.[15] The Co–Cl distance (both Co–Cl bonds are equal as required by crystallographic symmetry) at 2.262(6) Å is typically covalent {*e.g.* 2.296(3) and 2.261(4) Å in $[CoCl(C_{20}H_{44}N_{12}S_4)]_2[CoCl_4]$[16]}. The two platinum(II) planes fuse at the S • • • S axis at a hinge angle of 127.9(6)°. Our recent data on some intermetallic complexes indicate that this angle increases with the increasing size of the heterometal and hence with the M–S lengths.[17] The present data agree with this trend. The significance of this hinge angle is a subject of two recent studies.[17,18]

The crystal lattice of complex **3** shows two crystallographically distinct molecules of the complex with insignificant

**Table 1** Selected bond lengths (Å) and angles (°) for $[CoPt_2Cl_2(PPh_3)_4(\mu_3\text{-}S)_2]$ **2**

| | | | |
|---|---|---|---|
| Pt(1)–S(1) | 2.356(4) | Pt(1)–S(1a) | 2.340(3) |
| Pt(1)–P(1) | 2.301(4) | Pt(1)–P(2) | 2.257(4) |
| Co–Cl(1) | 2.262(6) | Co–S(1) | 2.359(4) |
| S(1)–Pt(1)–S(1a) | 80.5(1) | S(1)–Pt(1)–P(1) | 88.0(1) |
| S(1)–Pt(1)–P(2) | 172.5(1) | S(1a)–Pt(1)–P(1) | 168.5(1) |
| S(1a)–Pt(1)–P(2) | 92.5(1) | P(1)–Pt(1)–P(2) | 99.0(1) |
| Cl(1)–Co–Cl(1a) | 104.8(2) | Cl(1)–Co–S(1) | 120.3(1) |
| Cl(1)–Co–S(1a) | 115.5(2) | S(1)–Co–S(1a) | 80.0(1) |
| Pt(1)–S(1)–Pt(1) | 85.8(1) | Pt(1)–S(1)–Co | 81.1(1) |
| Pt(1)–S(1)–Co | 81.5(1) | | |

Symmetry position: a $-x, y, \frac{1}{2}-z$.

bonding variations (Fig. 2). Both contain a Pt–S–Pt triangular core with two phosphines *trans* and two carbonyls *cis* to the Pt–Pt bond (Table 2 and Fig. 3). With both platinum(I) spheres approximately planar, the molecule is essentially flat [mean deviation 0.067(6) Å]. The Pt–Pt distance [2.600(1) and 2.601(1) Å] is slightly shorter, and presumably stronger, than that in **4** [2.647(2) Å],[13] whereas the Pt–S bonds are marginally weaker [average 2.256(5) Å in **3** compared to 2.223(9) Å in **4**].

Two main issues concerning complexes **3** and **4** are the strengths of the Pt–Pt bonds and the relative positions of the phosphine and carbonyl ligands. To gain some insight into these aspects, we have turned to Fenske–Hall molecular orbital (MO) calculations.*[,19] These indicate a sizeable Pt–Pt interaction (in **3**) with an overlap population of 0.157. This value is, however, lower than that in $[Pt_4(\mu\text{-}O_2CMe)_8]$ in which the average overlap population is 0.235.[20] Possible reasons include the higher electron count for $Pt^I$, as well as the strong σ interaction of $PPh_3$ (compared to acetate) with Pt, which occurs at the partial expense of the Pt–Pt bond. It should be noted that the formation of the Pt–Pt bond can be accounted for qualitatively by the 16-electron rule for $Pt^I$. From a more theoretical perspective, since $Pt^I$ is $d^9$ and distorted square planar, for each Pt atom one would 'normally' expect one electron to occupy the d orbital that is metal–ligand antibonding.† The unfavourable effect is partially avoided by using the s and p orbitals: for Pt–Pt along the *z* axis and $Pt_2S$ in the *yz* plane, the major percent contributions to the HOMO 2 (the highest occupied molecular orbital is sulfur-based) are Pt(1) $d_{x^2-y^2}$ 6.04, $d_{yz}$ 2.09, s 5.96, $p_y$ 2.43, $p_z$ 15.16; Pt(2) $d_{x^2-y^2}$ 6.35, $d_{yz}$ 2.60, s 5.38, $p_y$ 2.04, $p_z$ 14.79.

In both complexes **3** and **4** the phosphines invariably prefer to be *trans* to the Pt–Pt bond whilst the carbonyls are *cis*. There appears to be no one obvious explanation for this preference apart from the higher symmetry thus obtained and the obvious steric problems if the phosphines were *cis* to the Pt–Pt bond. One possible rationalization uses a geometrical argument based on CO being a stronger π acceptor, as well as the premise that Pt–Pt and all platinum–ligand bonds are incorporated into a highly distorted square-planar framework at each Pt. With regard to the latter, the small S–Pt–Pt angles necessitate larger P–Pt–C angles. It can be easily shown, from straightforward geometrical considerations, that the *trans* L–Pt–Pt angles would be further from 180° than the *cis* L–Pt–Pt angles are from 90° [this is supported by the crystal structure: Pt(2)–Pt(1)–P(1) 156.8, Pt(1)–Pt(2)–P(2) 162.7, Pt(2)–Pt(1)–C(1) 99.1, Pt(1)–Pt(2)–C(2) 99.2°]. Owing to the symmetry of the Pt–Pt and platinum–ligand σ- and π-orbital interactions, angles of 180 and 90° for *trans* and *cis* ligands respectively are optimal for

* Mulliken population analysis was used to calculate overlap populations.

† The relevant electrons on the two Pt atoms would be expected to pair up, which presumes interaction of the orbitals on the two atoms.

**Table 2** Selected bond lengths (Å) and angles (°) for $[Pt_2(CO)_2(PPh_3)_2(\mu\text{-}S)]$ **3**

| | | | |
|---|---|---|---|
| Molecule A | | | |
| Pt(1)–Pt(2) | 2.5998(9) | Pt(1)–S(1) | 2.269(4) |
| Pt(1)–P(1) | 2.292(4) | Pt(1)–C(1) | 1.76(2) |
| Pt(2)–S(1) | 2.258(5) | Pt(2)–P(2) | 2.292(4) |
| Pt(2)–C(2) | 1.87(2) | O(1)–C(1) | 1.22(2) |
| O(2)–C(2) | 1.11(2) | | |
| Pt(2)–Pt(1)–S(1) | 54.7(1) | Pt(2)–Pt(1)–P(1) | 156.8(2) |
| Pt(2)–Pt(1)–C(1) | 99.1(6) | S(1)–Pt(1)–P(1) | 102.6(2) |
| S(1)–Pt(1)–C(1) | 153.6(7) | P(1)–Pt(1)–C(1) | 103.7(6) |
| Pt(1)–Pt(2)–S(1) | 55.1(2) | Pt(1)–Pt(2)–P(2) | 162.7(2) |
| Pt(1)–Pt(2)–C(2) | 99.2(5) | S(1)–Pt(2)–P(2) | 107.7(1) |
| S(1)–Pt(2)–C(2) | 154.1(5) | P(2)–Pt(2)–C(2) | 98.0(5) |
| Pt(1)–S(1)–Pt(2) | 70.1(1) | Pt(1)–C(1)–O(1) | 178(1) |
| Pt(2)–C(2)–O(2) | 179(1) | | |
| Molecule B | | | |
| Pt(3)–Pt(4) | 2.6008(8) | Pt(3)–S(2) | 2.270(4) |
| Pt(3)–P(3) | 2.287(4) | Pt(3)–C(3) | 1.85(3) |
| Pt(4)–S(2) | 2.253(5) | Pt(4)–P(4) | 2.298(4) |
| Pt(4)–C(4) | 1.89(2) | O(3)–C(3) | 1.15(3) |
| O(4)–C(4) | 1.08(2) | | |
| Pt(4)–Pt(3)–S(2) | 54.6(1) | Pt(4)–Pt(3)–P(3) | 157.6(2) |
| Pt(4)–Pt(3)–C(3) | 100.1(7) | S(2)–Pt(3)–P(3) | 103.0(2) |
| S(2)–Pt(3)–C(3) | 154.7(8) | P(3)–Pt(3)–C(3) | 102.3(7) |
| Pt(3)–Pt(4)–S(2) | 55.2(2) | Pt(3)–Pt(4)–P(4) | 159.8(2) |
| Pt(3)–Pt(4)–C(4) | 100.2(5) | S(2)–Pt(4)–P(4) | 104.6(1) |
| S(2)–Pt(4)–C(4) | 155.4(6) | P(4)–Pt(4)–C(4) | 100.0(6) |
| Pt(3)–S(2)–Pt(4) | 70.2(1) | Pt(3)–C(3)–O(3) | 177(2) |
| Pt(4)–C(4)–O(4) | 177(2) | | |

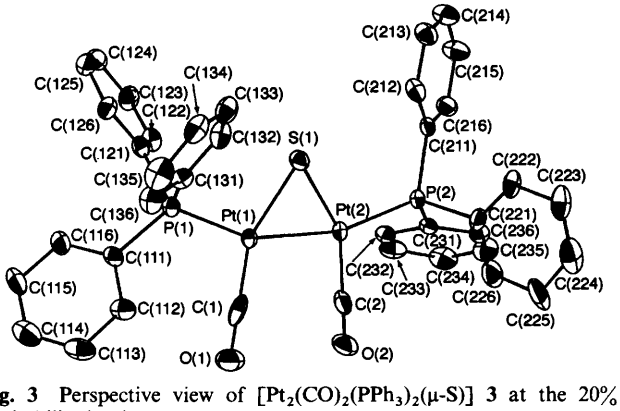


**Fig. 3** Perspective view of $[Pt_2(CO)_2(PPh_3)_2(\mu\text{-}S)]$ **3** at the 20% probability level

π back bonding. Since CO is a better π acceptor than $PPh_3$, and since the *cis* positions in the dimer are more favourable for π back bonding, the carbonyl understandably occupies these positions.

Finally, it may be the sulfur ligand is nucleophilic. In **3** the HOMO 3 is 48.44% S $p_y$ (see alignment described earlier), while the HOMO is 72.85% $p_x$.

As mentioned earlier, the stronger σ-donor ability and polarizability of phosphine (compared to CO) causes a weakening of the *trans* Pt–Pt bond. At the same time, phosphine is a weaker π acceptor; this is a 'disadvantage' to the Pt–Pt bond in the sense that π back donation reduces the net repulsive interactions between non-bonding d electrons on the metal. The latter effect is greater for a *trans* ligand. Not surprisingly, when one $PPh_3$ is swapped with the CO on the same Pt atom (everything else being held constant), the Pt–Pt overlap population increases from 0.157 to 0.170. At the same time, the Pt–P overlap population increases from 0.475 to 0.501, while those of Pt–C and Pt–S decrease from 0.550 to 0.500 and from 0.334 to 0.317 respectively. Curiously enough, for the two phosphines bound to the same Pt atom in **4**, the Pt–P bond *trans* to the Pt–Pt bond is shorter than the other bond (2.226 compared to 2.267 Å),[13] as well as the analogous bonds in **3**. This, along with reduced π acceptance due to one less CO, could account for the weaker, and hence longer, Pt–Pt bond in **4**. Thus, the final structures of **3** and **4**, as in all compounds, result from an overall optimization of all interactions;* in particular, stronger metal–ligand interactions are preferred to metal–metal interactions.

The observed loss of the heterometal atom in the conversion of complex **2** into **3** is reminiscent of the reported reductive desulfurization of **1** to **4** *via* the elimination of COS gas.[10] The elimination of the heterometallic fragment is probably an indication of the relative strengths of the Pt–S and Co–S bonds. This elimination cautions further that homogeneous catalytic reactions using a heterometallic cluster as the catalyst precursor do not necessarily involve a mixed-metal species as the active species especially when they are carried out under pressure.

## Experimental

All reactions were routinely performed under a pure argon atmosphere unless otherwise stated. All solvents were distilled and degassed before use. The complex $[Pt_2(PPh_3)_4(\mu\text{-}S)_2]$ was synthesized from *cis*-$[PtCl_2(PPh_3)_2]$ and $Na_2S{\cdot}9H_2O$ according to a literature method.[21] Elemental analyses were conducted in the Microanalytical Laboratory in the Department of Chemistry. The $^{31}P\text{-}\{^1H\}$ NMR spectra were recorded at 298 K on a Bruker ACF 300 spectrometer with $H_3PO_4$ as external reference, infrared spectra as KBr discs on a Perkin-Elmer 1600 FT-IR spectrophotometer. Conductivity was determined using a STEM Conductivity 1000 meter. Magnetic susceptibility was measured at 298 K on a Johnson Matthey magnetic susceptibility balance.

### Syntheses

**$[CoPt_2Cl_2(PPh_3)_4(\mu_3\text{-}S)_2]$ 2.** To a tetrahydrofuran (10 $cm^3$) suspension of $[Pt_2(PPh_3)_4(\mu\text{-}S)_2]$ (0.15 g, 0.1 mmol) was added with stirring a solution of $CoCl_2$ (0.013 g, 0.1 mmol) in thf (1 $cm^3$). The orange suspension dissolved rapidly to form a clear yellowish green solution which soon gave rise to a yellowish green precipitate. Stirring was continued for 30 min to ensure complete reaction. The precipitate was filtered off and purified by recrystallization from $CH_2Cl_2$–hexane to yield **2** as a yellowish green microcrystalline solid (0.103 g, 63%) (Found: C, 52.7; H, 3.8; Cl, 4.4; Co, 3.5; P, 7.4: Pt, 20.4; S, 4.0. $C_{76}H_{60}Cl_2CoP_4Pt_2S_2$ requires C, 52.9; H, 3.7; Cl, 4.3; Co, 3.6; P, 7.6; Pt, 23.9; S, 3.9%). $\delta_P(CDCl_3)$ 14.1 [t, $^1J$(P–Pt) 3679 Hz]. $\Lambda_m$ ($10^{-3}$ mol $dm^{-3}$, $CH_2Cl_2$) 3.3 $\Omega^{-1}$ $cm^2$ $mol^{-1}$. Magnetic moment $\mu = 4.79$ $\mu_B$. Single crystals were obtained by slow diffusion of hexane vapour into a solution of **2** in $CH_2Cl_2$.

**$[Pt_2CO_2(PPh_3)_2(\mu_3\text{-}S)]$ 3.** A suspension of complex **2** (0.163 g, 0.1 mmol) in thf (20 $cm^3$) was flushed with CO and stirred in a stainless-steel bomb cylinder of an autoclave (Parr T316ss reactor with magnetic drive) for 24 h at 80 °C under a carbon monoxide pressure of 45 psi which resulted in a clear yellowish green solution. This solution was added to hexane (50 $cm^3$) and the yellowish green precipitate, which contained an unknown cobalt compound, was filtered off. The yellow filtrate was evaporated to dryness under vacuum. The residue was dissolved in $CH_2Cl_2$–MeOH (1:3, 10 $cm^3$) and the solution filtered. The

* It is not definitively known why the Pt–S bonds are shorter in complex **4**. A possible clue lies in the relatively long Pt–P and Pt–C bonds *trans* to the Pt–S bonds. Note that when $PPh_3$ and CO were swapped in **3**, the Pt–P overlap population increased; this is not reflected in the *trans*(-S) Pt–P bond being shorter in **4**. Furthermore, calculations on **3** (modified) and **4**, both with the $Pt_2S$ core, indicate that the Pt–S overlap population [relevant to the $Pt(PPh_3)_2$ fragment in **4** and the analogous $Pt(PPh_3)(CO)$ fragment in **3**] is lower in **4** (0.330) than **3** (0.356). Thus, it is unlikely that CO has a higher ground-state *trans* influence.

**Table 3** Crystallographic data[a] for complexes $[CoPt_2Cl_2(PPh_3)_4(\mu_3\text{-}S)_2]$ **2** and $[Pt_2(CO)_2(PPh_3)_2(\mu\text{-}S)]$ **3**

| Formula | $C_{72}H_{60}Cl_2CoP_4Pt_2S_2$ | $C_{76}H_{60}O_4P_4Pt_4S_2$ |
|---|---|---|
| Crystal dimensions/mm | 0.4 × 0.08 × 0.06 | 0.5 × 0.38 × 0.04 |
| $M$ | 1633.32 | 2005.71 |
| Space group | $C2/c$ (no. 15) | $P2_1/n$ (no. 14) |
| $a$/Å | 20.176(7) | 17.797(3) |
| $b$/Å | 18.956(7) | 20.620(7) |
| $c$/Å | 17.517(5) | 19.078(4) |
| β/° | 92.97(3) | 98.28(2) |
| $U$/Å$^3$ | 6690.5 | 6928.3 |
| $D_c$/g cm$^{-3}$ | 1.62 | 1.92 |
| $F$(000) | 3204 | 3808 |
| μ/cm$^{-1}$ | 47.3 | 83.3 |
| Scan width | 1.35 + 0.35 tan θ | 0.6 + 0.35 tan θ |
| $hkl$ Ranges | 0–23, 0–21, −20 to 20 | 0–21, 0–24, −22 to 22 |
| Unique reflections measured | 6068 | 12 562 |
| Reflections with $F_o^2 \geqslant 3\sigma(F_o^2)$ | 3667 | 8479 |
| No. parameters | 375 | 811 |
| Goodness of fit, $S$[b] | 0.78 | 1.06 |
| $R$, $R'$[c] | 0.050, 0.061 | 0.053, 0.062 |
| $(\Delta/\sigma)_{max}$ | 0.03 | 0.59 |
| $(\Delta/\rho)_{max}$ | 2.23 | 4.80 |

[a] Details in common: monoclinic, $Z = 4$, $2\theta_{max} = 50°$. [b] $S = [\Sigma w(F_o - F_c)^2/(n - p)]^{\frac{1}{2}}$, $n$ = number of observed reflections, $p$ = number of parameters. [c] $R = \Sigma|F_o - F_c|/\Sigma F_o$, $R' = [\Sigma w(F_o - F_c)^2/\Sigma w F_o^2]^{\frac{1}{2}}$, $w = 1/[\sigma^2(F_o^2) + (0.020F_o)^2 + 1.00]$.

filtrate was allowed to evaporate in air slowly to give yellow crystals of **3** (0.027 g, 27%) (Found: C, 46.1; H, 3.2; P, 5.9; Pt, 34.5; S, 2.7. $C_{76}H_{60}O_4P_4Pt_4S_2$ requires C, 45.5; H, 3.0; P, 6.2; Pt, 38.9; S, 3.2%). $\nu_{CO}$ 2027vs and 1990s cm$^{-1}$. $\delta_P(C_6D_6)$ 24.1 [$^1J$(P–Pt) 3180, $^2J$(P–Pt) 148 Hz].

### Crystallography

All intensity data were collected on an Enraf-Nonius CAD4 diffractometer with graphite-monochromated Mo-Kα radiation (λ = 0.710 73 Å) and ω–2θ scan mode. Cell constants and orientation matrices for data collection were obtained from least-squares refinement using 21 reflections in the range $12 < \theta < 13°$ for complex **2**, and 25 reflections in the range $14 < \theta < 15°$ for **3**. A summary of the data collection and structure refinement parameters is given in Table 3. Intensity data were corrected for Lorentz-polarization effects. Empirical absorptions were based on a series of ψ scans. The structures of **2** and **3** were solved by the Patterson heavy-atom and direct method respectively. Both were refined by full-matrix least-squares techniques for all non-hydrogen atoms. Hydrogen atoms of the organic ligands were generated geometrically, assigned appropriate isotropic thermal parameters and allowed to ride on their parent carbon atoms; they were included in the refinement. All calculations were performed on a COMPAQ computer using the MOLEN PC[22] program package. Scattering factors were taken from Cromer and Waber.[23]

Atomic coordinates, thermal parameters, and bond lengths and angles have been deposited at the Cambridge Crystallographic Data Centre (CCDC). See Instructions for Authors, *J. Chem. Soc., Dalton Trans.*, 1996, Issue 1. Any request to the CCDC for this material should quote the full literature citation and the reference number 186/211.

## Acknowledgements

This work was supported by the National University of Singapore (NUS) (Grant RP 950695). H. L. thanks NUS for the award of a research studentship. A. L. T. is grateful to the National Science and Technology Board for a postdoctoral fellowship award, and the National Supercomputing Research Centre for use of its computing facilities and software.

## References

1 C. E. Briant, D. I. Gilmour, M. A. Luke and D. M. P. Mingos, *J. Chem. Soc., Dalton Trans.*, 1985, 851; D. I. Gilmour, M. A. Luke and D. M. P. Mingos, *J. Chem. Soc., Dalton Trans.*, 1987, 335.
2 C. E. Briant, T. S. A. Hor, N. D. Howells and D. M. P. Mingos, *J. Chem. Soc., Chem. Commun.*, 1983, 1118.
3 B. H. Aw, K. K. Looh, H. S. O. Chan, K. L. Tan and T. S. A. Hor, *J. Chem. Soc., Dalton Trans.*, 1994, 3177.
4 C. E. Briant, T. S. A. Hor, N. D. Howells and D. M. P. Mingos, *J. Organomet. Chem.*, 1983, **256**, C15.
5 W. Bos, J. J. Bour, P. P. J. Schlebos, P. Hageman, W. P. Bosman, J. M. M. Smits, J. A. C. van Wietmarschen and P. T. Beurskens, *Inorg. Chim. Acta*, 1986, **119**, 141.
6 M. Zhou, Y. Xu, L.-L. Koh, K. F. Mok, P.-H. Leung and T. S. A. Hor, *Inorg. Chem.*, 1993, **32**, 1875.
7 M. Zhou, Y. Xu, C.-F. Lam, L.-L. Koh, K. F. Mok, P.-H. Leung and T. S. A. Hor, *Inorg. Chem.*, 1993, **32**, 4660.
8 T. S. A. Hor, D.Phil. Thesis, University of Oxford, 1983.
9 B. N. Figgis, in *Comprehensive Coordination Chemistry*, eds. G. Wilkinson, R. D. Gillard and J. A. McCleverty, Pergamon, Oxford, 1987, vol. 1, ch. 6, pp. 271–274.
10 C.-H. Chin and T. S. A. Hor, *J. Organomet. Chem.*, 1996, **509**, 101.
11 D. G. Evans, M. F. Hallam, D. M. P. Mingos and R. W. M. Wardle, *J. Chem. Soc., Dalton Trans.*, 1987, 1889.
12 J. Chatt and D. M. P. Mingos, *J. Chem. Soc. A*, 1970, 1243.
13 M. C. Baird and G. Wilkinson, *J. Chem. Soc. A*, 1967, 865; A. C. Skapsi and P. G. H. Troughton, *J. Chem. Soc. A*, 1969, 2772.
14 J. C. Jeffery, M. J. Parrott and F. G. A. Stone, *J. Organomet. Chem.*, 1990, **382**, 225.
15 F. Cecconi, C. A. Ghilardi, S. Midollini, A. Orlandini and P. Zanello, *Polyhedron*, 1986, **5**, 2021.
16 M. Gostojic, V. Divjakovic, V. M. Leovac, B. Ribar and P. Engel, *Cryst. Struct. Commun. A*, 1982, **11**, 1209.
17 A. L. Tan, M. L. Chiew and T. S. A. Hor, *J. Mol. Struct. (TheoChem.)*, 1996, in the press.
18 M. Capdevila, W. Clegg, P. González-Duarte, A. Jarid and A. Lledós, *Inorg. Chem.*, 1996, **35**, 490.
19 M. B. Hall and R. F. Fenske, *Inorg. Chem.*, 1972, **11**, 768.
20 A. L. Tan, P. M. N. Low, Z.-Y. Zhou, W. Zheng, B. M. Wu, T. C. W. Mak and T. S. A. Hor, *J. Chem. Soc., Dalton Trans.*, 1996, 2207.
21 R. Ugo, G. La Monica, S. Cenini, A. Segre and F. Conti, *J. Chem. Soc. A*, 1971, 522.
22 MOLEN, An Interactive Structure Solution Procedure, Enraf-Nonius, Delft, 1990.
23 D. T. Cromer and J. T. Waber, *International Tables for X-Ray Crystallography*, Kynoch Press, Birmingham, 1974, vol. 4, Table 2.2B.

*Received* 30*th April* 1996; *Paper* 6/03037H